Synthesis of Chromite for Subsequent Carburization by Methane-Hydrogen Gas Mixture

Vincent Canaguier, Ingeborg-Helene Svenum and Leiv Kolbeinsen

Abstract The syntheses of stoichiometric iron chromite and chromites with chosen impurity content have been developed using the induction skull melting technique. The aim for this synthetic material is to obtain pure samples to study the carburization by methane-hydrogen gas mixtures. For each synthesis, the parameters influencing the skull melting experiment have been considered. The product phases have been analyzed using X-Ray Diffraction (XRD), Scanning Electron Microscopy (SEM), Energy-Dispersive X-ray Spectroscopy (EDS) and X-ray Photoelectron Spectroscopy (XPS). The synthetic material was subsequently pelletized and sintered in argon. The use of excess iron was found to improve the quality of the final product as well as to help the melting. The difference in magnesium content between first and last solids formed seem to indicate a segregation phenomenon, while no evidence could support a similar trend for aluminum substitution in chromite.

Keywords Synthesis · Chromite · Skull melting

Introduction

Mineral ores are the starting point for most metal production processes. These ores often contain a wide range of impurities in addition to the valuable oxides. It is known that the composition of these ores vary from deposit to deposit, and also within a single deposit. For chromite ores, which are the focus of this article, significant variations can be observed. The contents of diverse oxides, such as: Cr_2O_3, FeO, Fe_2O_3, Al_2O_3, MgO, SiO_2 and CaO in natural chromites are subject to

V. Canaguier (✉) · L. Kolbeinsen
NTNU, Norwegian University of Science and Technology,
Alfred Getz vei 2, Trondheim 7491, Norway
e-mail: vincent.y.canaguier@ntnu.no

I.-H. Svenum
SINTEF Materials and Chemistry, Høgskoleringen 5, Trondheim 7034, Norway

J.-Y. Hwang et al. (eds.), *8th International Symposium on High-Temperature Metallurgical Processing*, The Minerals, Metals & Materials Series,
DOI 10.1007/978-3-319-51340-9_2

important fluctuations [1]. These make the investigation of their individual effect, e.g. on reduction rates, particularly complicated as it is not possible to vary one oxide content at a time using natural ores.

Chromites of various compositions have been investigated in several former studies using synthetic materials. Other studies focused on the synthesis of these oxides in a pure form. Solid-state synthesis, using various protocols, was used to produce synthetic chromite ($FeCr_2O_4$) [2–4] and synthetic magnesiochromite ($MgCr_2O_4$) [2]. In addition, Qayyum et al. synthetized various compositions of the $(Fe, Mg)(Cr, Al)_2O_4$ solid solution in solid-state [3], while $(Fe, Mg)(Fe, Cr, Al)_2O_4$ solid solution synthesis was studied by Wu et al. [5].

The work presented in this article aimed at developing a liquid state synthesis route allowing the production of large quantities of material at once and in a short time. A high production capacity is required to allow pelletization and sintering of the material prior to reduction and carburization experiments. The quality and variability of the composition of the synthesized oxides are used to evaluate this synthesis route.

Experimental Details

The Skull Melting technique, using a cold crucible induction furnace, is utilized for the synthesis of the $(Fe_{1-x}Mg_x)(Cr_{1-y}Al_y)_2O_4$ solid solution samples.

Apparatus

The equipment used for the synthesis is a cold crucible induction furnace. It consists in two parts: a high frequency induction coil supplied by Farfield Electronics PTY Ltd (750 kHz, 75 kVA) for the heating and a water-cooled copper crucible supplied by ANSTO. The control of the furnace is performed by changing the current input in the induction coil. A schematic of the equipment is given in Fig. 1.

The copper crucible is cylindrically shaped, and its wall is built from “fingers” separated from each other by an interstitial space. The inside and the top surfaces of the crucible are coated before use with a boron-nitride coating applied either as a paste or with a spray. A top view schematic of a loaded crucible is given in Fig. 2. The mass load capacity is then determined by the shape and density of the raw materials and varies between 200 and 300 g.

The inside of the furnace, delineated by the external glass tube, is evacuated by a rotary pump. The atmosphere can be replaced by an inert gas. The temperature measurements are performed by a spectropyrometer type FMP 2 from FAR Associates.

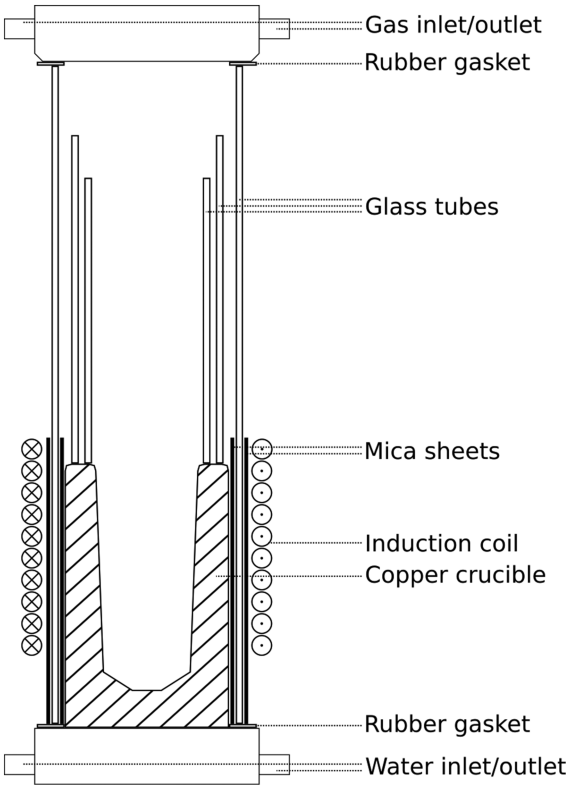

Fig. 1 Schematics of the cold crucible induction furnace with a cut view

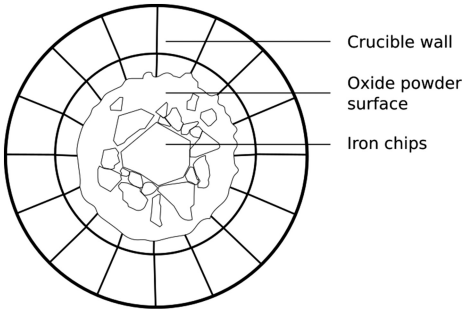

Fig. 2 Schematics of the crucible and loading with a top view

Chromite Solid Solution Synthesis

The reactants used for the synthesis are Cr_2O_3 powder (purity 98%), Fe_2O_3 powder (size $\leq$ 5 μm, purity $\geq$ 99%), pure Fe pieces (chips, purity 99.98%), and Al_2O_3 powder (size $\leq$ 10 μm, purity $\geq$ 99.5%). The quantities are based on a stoichiometric reaction synthesis plus excess iron if relevant. The gas atmosphere used is argon, blown in at 1.19 NL/min.

Table 1 Synthesis parameters for the $(Fe_{1-x}Mg_x)(Cr_{1-y}Al_y)_2O_4$ samples

Ref.	Sample	Power [kW]	Fe [g]	Fe^a_{xs} [g]	Fe_2O_3 [g]	Cr_2O_3 [g]	Al_2O_3 [g]	MgO [g]
1	x = 0, y = 0	67.50[b]	16.74	0	47.56	135.87	0	0
2	x = 0, y = 0	52.50	13.30	0	38.03	108.63	0	0
3	x = 0, y = 0	63.75	16.63	0	47.48	135.85	0	0
4	x = 0, y = 0	63.75	16.63	4.08	51.76	135.81	0	0
5	x = 0, y = 0	63.75	16.61	2.00	47.57	135.81	0	0
6	x = 0, y = 0.25	63.75	17.65	0	50.38	107.97	24.12	0
7	x = 0.25, y = 0	63.75	12.92	0	36.96	140.72	0	9.34
8	x = 0.25, y = 0	63.75	12.93	7.35	36.99	140.80	0	9.50

[a] Fe_{xs} is the iron excess added with regard to the stoichiometric composition
[b] Reduced to 52.50 kW during the experiment due to splashing

The oxide powders were mixed in a plastic bag and were placed and packed in the crucible. The iron chips were placed on the top of the oxides so that the biggest chips were in the center of the crucible and a maximum of the surface was covered. For several stoichiometric chromite samples (x = 0, y = 0) and one chromite-magnesiochromite solid solution sample (x = 0.25, y = 0), excess iron was added to ensure good melting. A sketch of the iron placement is given in Fig. 2. The synthesis parameters for the $(Fe_{1-x}Mg_x)(Cr_{1-y}Al_y)_2O_4$ solid solution samples are provided in Table 1.

Analyses

The composition of the synthesized phases was analyzed by X-ray diffraction (XRD) using a Bruker D8 DaVinci. Scanning ranges of $2\theta = 5–60°$ and $2\theta = 15–75°$ were used. The radiation was obtained from a copper anode. The peaks obtained were compared to the Powder Diffraction File (PDF) database.

Parts of the sample representative of the section of the synthesis product were embedded in epoxy and polished using SiC paper and diamond suspensions. These samples mounted in epoxy were cleaned with ethanol, partly wrapped in aluminum and degassed overnight. Secondary electron (SE), backscattered electron (BSE) and energy-dispersive x-ray spectroscopy (EDS) images were obtained using a field emission scanning electron microscope (FESEM Zeiss Supra or FESEM Zeiss Ultra). X-ray photoelectron spectroscopy (XPS) analysis was performed using a Kratos Axis Ultra spectrometer with a monochromatic Al Kα source. Individual core levels were measured with a pass energy of 20 eV. XPS analysis was carried out on powder samples pressed onto carbon tape.

Pelletizing and Sintering

Once the material has been synthesized and verified, it was crushed and pelletized without binding additives. The pellets were sized between 1 and 1.6 mm of diameter. After drying the pellets were sintered in argon at 870 °C for 2 h.

Results and Discussion

Product Appearance

The synthesis product was first observed with the naked eye to evaluate the success of the melting. A first criterion for a successful melting is the absence of crust on the top of the crucible. When the iron chips placed on the top of the charge melt, surrounding oxides will start melting too, and ultimately a molten bath is formed in the bottom of the crucible. If oxides are left on the top they might fall down in the melt and dissolve into it. However, if these oxides heated by the radiating iron chips sinter before the formation of the melt, a part of the oxides is left unaffected and hence does not fall into the melt. This will damage the product's composition as the stoichiometry of the reaction cannot be fulfilled. Pictures of a sample after synthesis and of a sintered oxide crust are given in Fig. 3.

To solve the crust formation problem, excess iron is used. Iron, when melting, pierces the oxide charge. With extra iron, and a good spread of the iron chips on the oxide charge surface, the crust is avoided. The downside is that the stoichiometry is once more at risk. But from a practical point of view, it is easier to remove extra iron that will form a distinct product phase than to remove M_2O_3 phases within the spinel solid solution. In addition to facilitate the melting, having excess iron is useful to compensate for the losses due to splashing.

All meltings except one were successful. The chromite synthesis (x = 0, y = 0) carried out at 70% power failed and only a small fraction of the reactants melted. This sample evidenced the minimum requirements in terms of power input.

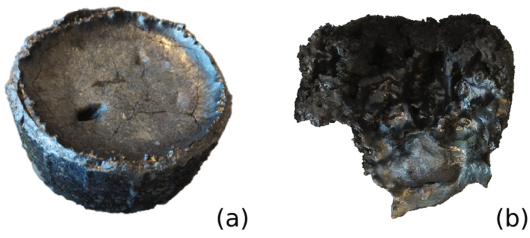

Fig. 3 Pictures of samples after synthesis: **a** Chromite sample (x = 0, y = 0). **b** Unreacted crust in a chromite-magnesiochromite synthesis experiment (x = 0.25, y = 0)

X-Ray Diffraction Analysis

The crystal structure was analyzed for each sample using XRD. The detected major and minor phases are reported in Table 2. The phases mentioned in the table are not necessarily present in the whole sample, as different part of the product were crushed down and analyzed independently. However, it shows the deviations from the expected material. The sample n°2 was discarded due to limited melting.

The sample n°1 shows a lot of unreacted chromium oxide which can be explained by two phenomena: the losses of pure iron due to splashing, and the subsequent modification of the power input. The sample n°3 showed the same trend, to a lower extent, even though the power input was reduced from the start and kept constant. The undesired phases were observed in small quantities as seen in samples n°4 and 5 only when iron is added. Concerning sample n°6, some unreacted M_2O_3 phase was observed, in addition to a dominant spinel phase. The main peaks fit to the pattern of $Fe(Cr_{1.4}Al_{0.6})O_4$ whose composition is close to the target. The minor phases left are a solid solution of aluminum and chromium oxide. For the sample n°7 large amounts of crust were observed which explains why some iron and chromium oxide were left unreacted. The spinel composition was found to be close to $(Fe_{0.67}Mg_{0.33})Cr_2O_4$, which makes sense given the unreacted iron in the sample. For the sample n°8, the patterns showed peaks matching the compositions of $(Fe_{0.91}Mg_{0.09})Cr_2O_4$ (inner sample) and $(Fe_{0.76}Mg_{0.24})Cr_2O_4$ (border sample). Traces of iron were observed by XRD analysis, but large amounts were remove before the crushing.

These observations have to be considered carefully as the different compositions of the spinel solid-solution studied are not easily distinguishable by XRD analysis.

Table 2 X-ray diffraction results for the $(Fe_{1-x}Mg_x)(Cr_{1-y}Al_y)_2O_4$ samples

Ref.	Sample	Power [kW]	Crust (Y/N)	Major phases	Minor phases
1	x = 0, y = 0	67.50[a]	N	$FeCr_2O_4$; Cr_2O_3	FeO
3	x = 0, y = 0	63.75	N	$FeCr_2O_4$; Cr_2O_3	–
4	x = 0, y = 0	63.75	N	$FeCr_2O_4$	Fe
5	x = 0, y = 0	63.75	N	$FeCr_2O_4$	Cr_2O_3
6	x = 0, y = 0.25	63.75	Y	$Fe(Cr_{1.4}Al_{0.6})O_4$	$(Cr_{1.25}Al_{0.72})O_3$
7	x = 0.25, y = 0	63.75	Y	$(Fe_{0.67}Mg_{0.33})Cr_2O_4$; Cr_2O_3;Fe	–
8	x = 0.25, y = 0	63.75	N	$(Fe_{0.91}Mg_{0.09})Cr_2O_4$; $(Fe_{0.67}Mg_{0.33})Cr_2O_4$; Fe[b]	–

[a]Reduced to 52.50 kW during the experiment due to splashing

[b]Only traces were detected by XRD but large amounts were removed before the analysis

However, the addition of pure iron seemed generally beneficial to the synthesis. For the samples n°4 and 5, where the iron addition was moderate, the product is very close to the desired composition. In the sample n°8 where a large amount of excess iron was necessary, a good part can be recovered before further processing of the ores. Also, within sample n°8, whose composition was analyzed close to the edge and close to the center, different patterns fitted the observed peaks. This suggests a different content in magnesium across the sample and is further investigated by elemental analysis.

SEM Imaging, EDS and XPS Analysis

The samples n°5, 6 and 8, which are considered the most successful based on their composition (x = 0, y = 0), (x = 0.25, y = 0) and (x = 0, y = 0.25) respectively are studied by electron microscopy. XPS analysis was also performed on a nominal $FeCr_2O_4$ sample. The obtained XPS spectra is consistent with a Fe/Cr ratio of 0.48 confirming the bulk composition. A picture of sample n°5 obtained using a backscattered electron detector is shown in Fig. 4. Further EDS analysis confirm that the bulk is a chromite spinel phase, but some impurities are also present. In sample n°5 and 8, a metallic Fe–Cr alloy phase and a FeO phase have been evidenced in addition to the spinel. In sample n°6, a $(Cr, Al)_2O_3$ phase was evidenced in addition to FeO and a Fe–Cr alloy.

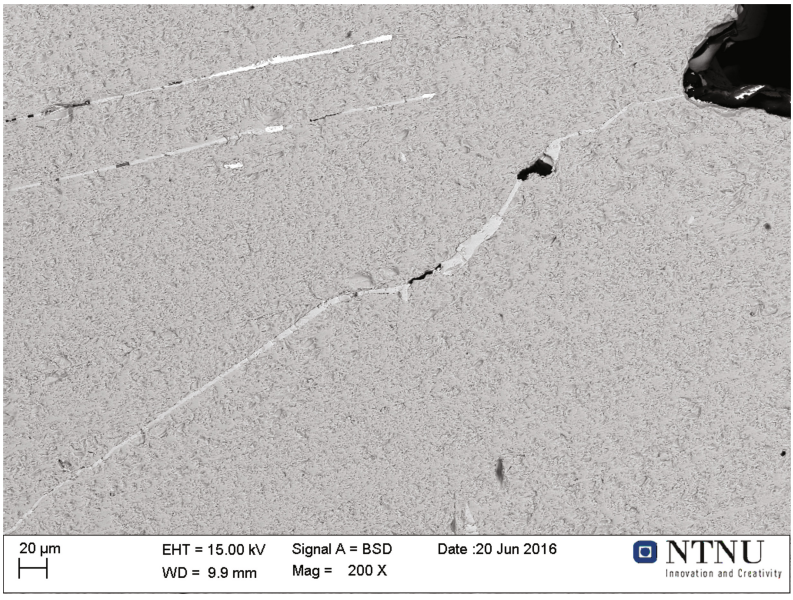

Fig. 4 Picture of a chromite sample (x = 0, y = 0)

Table 3 Metallic ratios from EDS measurements and targeted values for the $(Fe_{1-x}Mg_x)(Cr_{1-y}Al_y)_2O_4$ samples

Ref.	Sample	(Fe + Mg)/(Cr + Al) [0.500]	Al/Cr [0.333]	Mg/Fe [0.333]
5	x = 0, y = 0	0.427–0.457	–	–
6	x = 0, y = 0.25	0.456–0.456	0.313–0.305	–
8	x = 0.25, y = 0	0.452–0.426	–	0.420–0.254

Point analysis were carried out on the samples to verify the metal ratios within the spinel phase. Two sets of point, near the center of the sample and near the edge, have been measured. The concept was to investigate whether a possible compositional gradient in aluminum or magnesium content exist between the first and last solid phases formed. The average metallic ratios are given in Table 3. The first value represents the average ratio for the edge sample (first solid), while the second value is the average for the center sample (last solid). The value in square brackets is the targeted metallic ratio. From these measurements, only the magnesium to iron ratio is distinct enough and may show a segregation phenomenon. The difference between the Fe/Cr ratio given by XPS and EDS for sample n°5 could be explained by the relatively low accuracy of EDS measurements.

Conclusions

Synthetic chromite, chromite-hercynite and chromite-magnesiochromite have been synthesized successfully by induction skull melting of pure reagents. The formation of a crust of sintered materials was found to be the foremost cause of failure during the synthesis, but addition of iron in excess facilitates the melting.

The XRD studies showed that the product phase is, to a large extent, the expected spinel phase. Though, the electron microscopy showed variations in the magnesium content within the spinel solid solution that may be attributed to a segregation phenomenon. Impurities such as FeO and a metallic phase are also detected by electron microscopy.

Acknowledgements This work was financed by the Norwegian Research Council (NRC-project 233825) through the CORALSEA project. The authors would also like to thank Edith Thomassen and Ingeborg Solheim for the pellet preparation.

References

1. J.F. Papp, B.R. Lipin, “Chromium” (Open-File Report 01-381, U.S. Geological Survey, 2001)
2. S. Klemme, H.St.C. O’Neill, W. Schnelle, E. Gmelin, The heat capacity of $MgCr_2O_4$, $FeCr_2O_4$, and Cr_2O_3 at low temperatures and derived thermodynamic properties. Am. Mineral. **85**, 1686–1693 (2000)

3. M.A. Qayyum, D.A. Reeve, Reduction of chromites to sponge ferrochromium in methane-hydrogen mixtures. Can. Metall. Q. **15**(3), 193–200 (1976)
4. N.S. Sundar Murti, V. Seshadri, Kinetics of reduction of synthetic chromite with carbon. Trans. Iron Steel Inst. Jpn. **22**(12), 925–933 (1982)
5. X.R. Wu, C. Chen, H.H. Lü, L.S. Li, Synthesis, structure characterization and magnetic property of $(Mg_{1-y}Fe_y)(Al_{0.4}Cr_xFe_{1.6-x})O_4$ spinel solid solution. *Material Science and Environmental Engineering*, ed. by Ping Chen (Wuhan, China: International Conference on Material Science and Environmental Engineering, 2015), pp. 109–113

http://www.springer.com/978-3-319-51339-3

8th International Symposium on High-Temperature Metallurgical Processing

Hwang, J.-Y.; Jiang, T.; Kennedy, M.W.; Yucel, O.; Pistorius, P.; Seshadri, V.; Zhao, B.; Gregurek, D.; Keskinkilic, E. (Eds.)

2017, XXII, 818 p. 421 illus., Hardcover
ISBN: 978-3-319-51339-3